JVSTB
JOURNAL OF VACUUM SCIENCE AND TECHNOLOGY B

Production of focused, lowenergy, hydrogenion beams using a Colutron ion source

Bruce L. Cain, David N. Ruzic, and Robert Bastasz

Citation: J. Vac. Sci. Technol. B **6**, 485 (1988); doi: 10.1116/1.584047
View online: http://dx.doi.org/10.1116/1.584047
View Table of Contents: http://avspublications.org/resource/1/JVTBD9/v6/i1
Published by the AVS: Science & Technology of Materials, Interfaces, and Processing

Production of focused, low-energy, hydrogen-ion beams using a Colutron ion source

Bruce L. Cain and David N. Ruzic
Department of Nuclear Engineering, University of Illinois, Urbana, Illinois 61801

Robert Bastasz
Sandia National Laboratories, Livermore, California 94550

(Received 27 May 1987; accepted 26 August 1987)

An ion beam decelerator for energies down to 5 eV is described. The decelerator is a Menzinger retardation system that has been modified according to the results of calculations using a ray tracing model to optimize lens geometry. Performance tests of the decelerator demonstrate that H_2^+ beams with currents $\geqslant 20$ nA can be obtained with a spot size adjustable from 0.5 to 10 mm using a beam raster system.

I. INTRODUCTION

The production and use of low-energy ions (< 100 eV) for basic surface physics research is of increasing interest to the technical community. Fusion energy researchers have found that low-energy, hydrogenic ions impinging upon first-wall and divertor/limiter surfaces strongly affect fusion fuel recycling processes and plasma impurity levels.[1,2] Laboratory measurements using low-energy hydrogen beams are needed to identify the physical processes responsible for these effects. In the microelectronics industry, which utilizes various types of low-energy plasma processes in the fabrication of semiconductor devices, the understanding of fundamental low-energy ion/surface interactions is important in the further development of these techniques.[3] The phenomena of interest include ion/surface accommodation, reflection of ions from surfaces, sputtering of surface material, and implantation/diffusion of incident ions into materials. To date, much of the knowledge about these low-energy processes results from numerical modeling and extrapolation from higher-energy experiments rather than from direct observation. Based on the sparsity of low-energy ion/surface data, and the importance of fully understanding this interaction regime, the interest in producing low-energy ion beams for surface studies is certainly justified.

In order to experimentally study low-energy ion/surface interactions, a well-characterized ion beam is necessary. This paper describes the design, construction, and performance of such a low-energy ion beam system. A Colutron[4] ion source was used to provide an initial beam of hydrogen ions, which was then decelerated to the desired lower energy. The success of this approach depends upon the decelerator stage design, which is described in detail.

II. ION SOURCE AND BEAM SYSTEM

The Colutron ion source, shown in Fig. 1, uses an arc discharge between a hot cathode (filament) and an anode to produce positive ions for extraction. The anode, filament, and discharge chamber are biased positive with respect to a grounded ion extraction lens located near an orifice in the arc discharge anode. This bias provides the primary energy of the extracted beam. The beam is then focused with an einzel lens arrangement through an $E \times B$ velocity filter (Wein-type).[5] At the Colutron exit port, the ion beam at a primary energy of a few keV is both focused and mass filtered. The advantages to using this type of source for surface studies are a low-ion-beam energy spread (typically < 1 eV), good mass filtering ability ($M/\Delta M \approx 200$–300), and a focused beam spot (0.1–1 mm diameter).[4]

Additional ion optics are usually required to further refine the beam. Figure 2 shows the utilization of the Colutron source in a secondary ion mass spectrometry (SIMS) apparatus,[6] where primary beam energies in the keV range are used. The differential pumping chamber contains horizontal deflection plates which deflect the beam 3°–5° to exit apertures leading into an analysis chamber. This deflection separates the ion beam from collimated neutral atoms, which cannot be removed by the Wein filter. Other ion optic components include a final focusing einzel lens and X–Y raster plates.

The raster plates provide important capabilities. First, by varying the magnitude of the raster voltage, the effective beam area can be selected. The narrow source beam is rastered over a rectangular area, which can serve to clean a sample. More importantly, it provides a uniform ion current density over the rastered area. Hence, the details of the source beam current-density profile are not critical. Second, the raster capability can be utilized to image the rastered area. By synchronizing the sweep of a video monitor with the raster scan and driving the video intensity with the current collected by the target, an image of the exact raster area can be displayed. The apparent current collected by the target is modulated by local differences in secondary-electron emission. These differences are amplified to obtain contrast in the video image.

III. LOW-ENERGY BEAM REQUIREMENTS

By simply reducing the primary beam energy, low-energy beams can be produced. However, transport losses over the distance from the source to target (> 1 m) are excessive. In order to obtain beam energies below 200 eV with acceptable intensity, it is best to decelerate a higher-energy beam to the desired low energy near the target. This can be accomplished

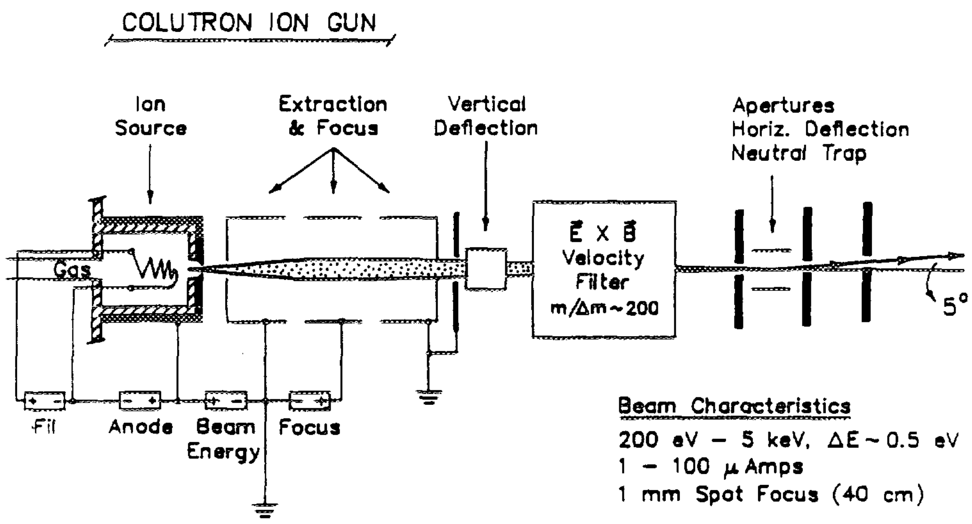

FIG. 1. Colutron ion gun components and neutral trap deflection system.

by inserting a decelerator stage in the beam line. Anticipating the beam quality requirements of ion/surface experiments, the goal of obtaining low-energy ions must be coupled to the following constraints on decelerator stage performance:

(1) It is important to retain the rastering and imaging capability in the beam system. Rastering makes it possible to vary the irradiation area, maintain uniform current density, and control beam position on the target.

(2) The decelerated beam characteristics should be independent of the sample geometry and material. Hence, it is important to maintain a field-free region near the target, so that different sample shapes can be used without having to recalibrate the beam optics.

(3) A beam size of < 1 mm and a beam current > 10 nA on target are needed throughout the energy range of the system.

IV. DECELERATOR STAGE DESIGN

An initial attempt was made to use a standard decelerator stage without modification. A Menzinger decelerator assembly[7] was installed in the analysis chamber along with a set of X–Y raster plates. As shown in Fig. 3, the decelerator consists of a set of six lens elements which serve to decelerate the beam and provide a final focusing lens at target potential. Lens element 1, a guard ring, was not used; lens element 2 is a grounded aperture, while lens elements 3 and 4 provide a two-stage energy reduction (or deceleration) to final beam energy. Lens elements 4, 5, and 6 form a einzel lens near the target. Lens elements 4 and 6 are maintained at the same potential as the target so that all beam energy reduction occurs within the decelerator, leaving the target vicinity field-free. The X–Y raster plates precede the decelerator lens assembly allowing the beam to be rastered at the primary beam energy and the final lens to have a short working distance.

A Faraday cup and beam scanning probe attached to the target holder were used to measure beam current and current-density profiles for the decelerator assembly of Fig. 3. Initial results showed that, although the beam current was adequate down to energies of 50 eV, the beam focus was poor. It was not possible to verify rastered spot size via the imaging system. An inspection of the decelerator geometry

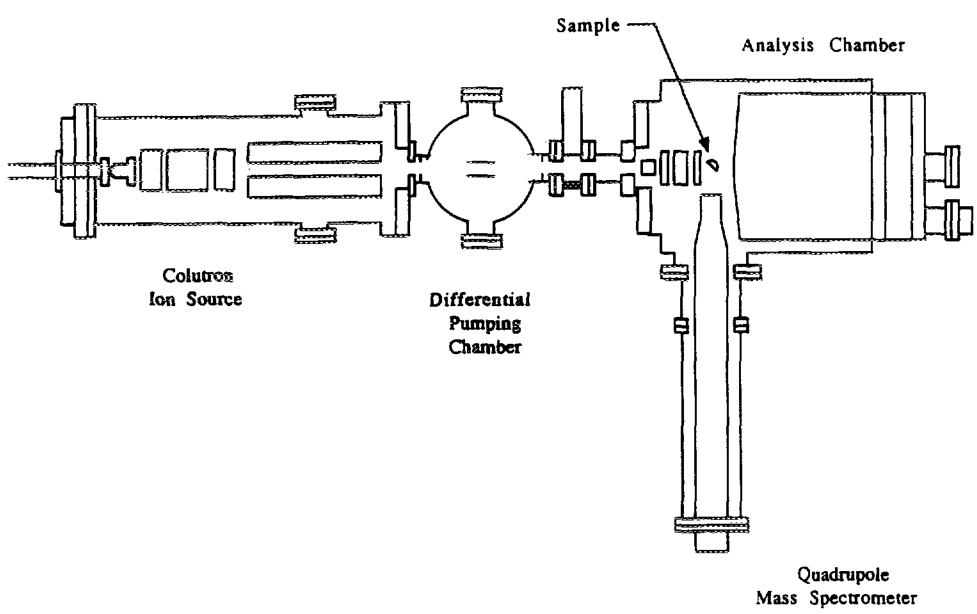

FIG. 2. Colutron ion gun and SIMS apparatus used for low-energy beam experiments. A beam deflection of 3°–5° in the pumping chamber is not shown.

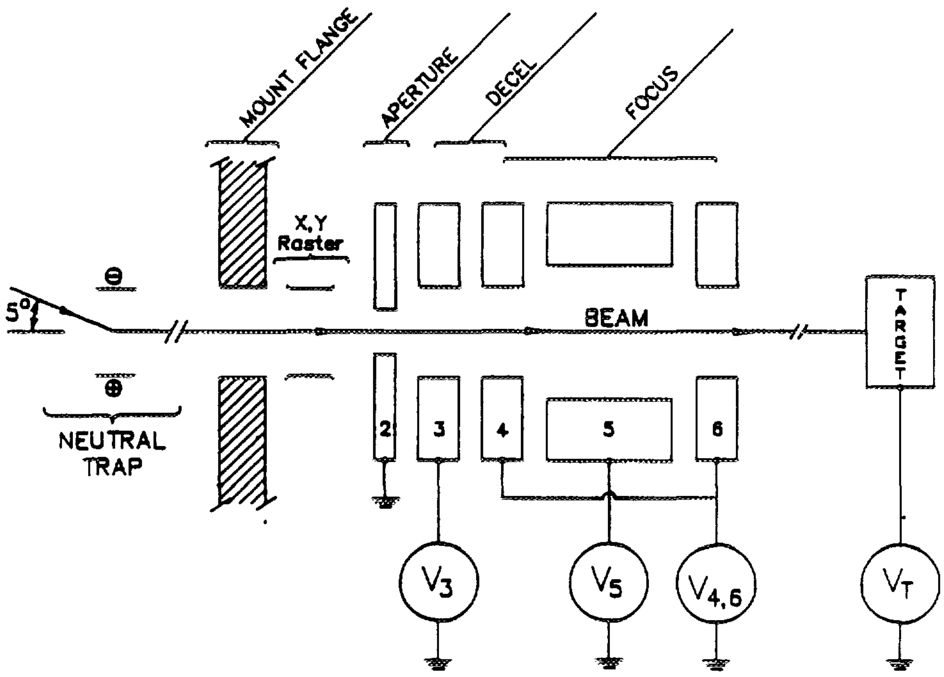

FIG. 3. Decelerator stage detail.

indicated that the probable cause of misfocusing was the asymmetry of the beam path through the lens elements. When the beam is rastered, the beam path is deflected off axis and nearly strikes lens elements 2 and 6 when the rastered area covers the target.

From these results it was clear that a larger bore diameter decelerator was needed. However overenlargement could reduce the effectiveness of the stage. In order to quantify the effects of changing the lens geometry, a charged particle (electron or ion) ray tracing program[8,9] was used to model the decelerator lens system. The program allows input of lens system geometry, potentials, and beam initial conditions (mass, energy, initial direction, and number of rays), then performs a three-dimensional Laplace paraxial ray analysis which traces the path of rays through the decelerator to the target. The calculations include the effects of beam space charge and self-magnetic field. A program plot is shown in Fig. 4 for a 1-keV beam with no deceleration using the geometry of Fig. 3. The action of the raster system is modeled by specifying a common start direction for a group of rays. Figure 4 depicts a "freeze frame" of the beam path for a deflection of 4.1 mm away from the lens axis. The vertical lines between lens elements are equipotential surfaces, where rotational symmetry about the Z axis is assumed. In Fig. 4, with no beam deceleration, focusing by the einzel lens is evident as all the rays converge to a point. In this case, moving the target to the focal point would produce a focused beam on the target since this region is field-free. In every case modeled, the einzel lens was operated in the retard/accel mode, the total beam current was set at 0.5 μA, and the raster direction was set to simulate maximum raster amplitude.

When the decelerator is modeled to produce a 1-keV-decelerated beam (1700-V primary potential—700-V decel-

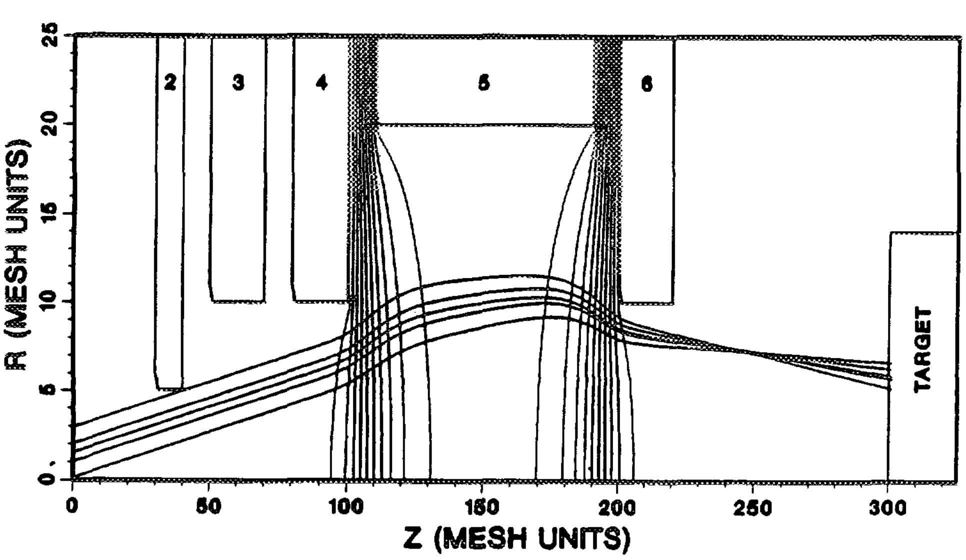

FIG. 4. Model plot of ray paths through decelerator of Fig. 3 for 1-keV beam with no deceleration. Experimentally determined lens potentials are used in this case as input parameters to the code. Various equipotentials are also shown.

eration potential), poor focus is obtained, as shown in Fig. 5(a), and the beam actually strikes lens element 6. Further increases in focus potential on lens element 5 move the beam out of contact, as shown in Fig. 5(b), but spot focus on the target is not possible. Numerous modeling calculations confirm the experimental observation that the original geometry cannot produce a beam that is at once decelerated, focused, and rastered over the entire target.

In subsequent calculations, the bore diameters of lens elements 2 through 6 were changed, in various combinations, to arrive at a geometry which would allow good focusing at maximum raster amplitude. A beam decelerated to 1 keV was used in most cases. Figure 6(a) shows the results for a constant bore diameter of 1.27 cm, where spot focusing is obtained. Of concern with this geometry, however, was the possible leakage of field lines into, or from, the raster plate region. The raster plates were not included in the model calculations because they lack cylindrical symmetry. Instead, additional calculations were used to determine the minimum diameter each lens element could have and still provide an unimpeded, focused beam. Figure 6(b) shows the final selected design, where spot focusing is achieved and lens element 2 still performs its aperture function.

V. PERFORMANCE TESTS

A decelerator assembly, with bore diameters of Fig. 6(b), was installed in the analysis chamber and tested to determine its performance in producing low-energy, hydrogen-ion beams (H_1^+, H_2^+, or H_3^+). Emphasis was placed on maximizing beam intensity on the target, via Faraday cup measurements, and on obtaining a good raster image of the beam profiling probe. Figure 7(a) is a plot of beam current as a function of the decelerated beam energy. At 5 eV, the current observed on target was $\approx$20 nA. At beam energies above 10 eV, a good raster image of the profiling probe was obtained through fine adjustment of the final-focus einzel lens potential. Figure 7(b) shows beam profiles, in the X scan direction with no beam raster, for decelerated beam energies of 5, 25, and 200 eV. The beam profiles demonstrate the ability to focus low-energy beams to spot diameters <0.5 mm. However, the specific profile for a given energy could be changed considerably by relatively small voltage adjustments on the final-focus einzel lens. Hence, these profiles are considered

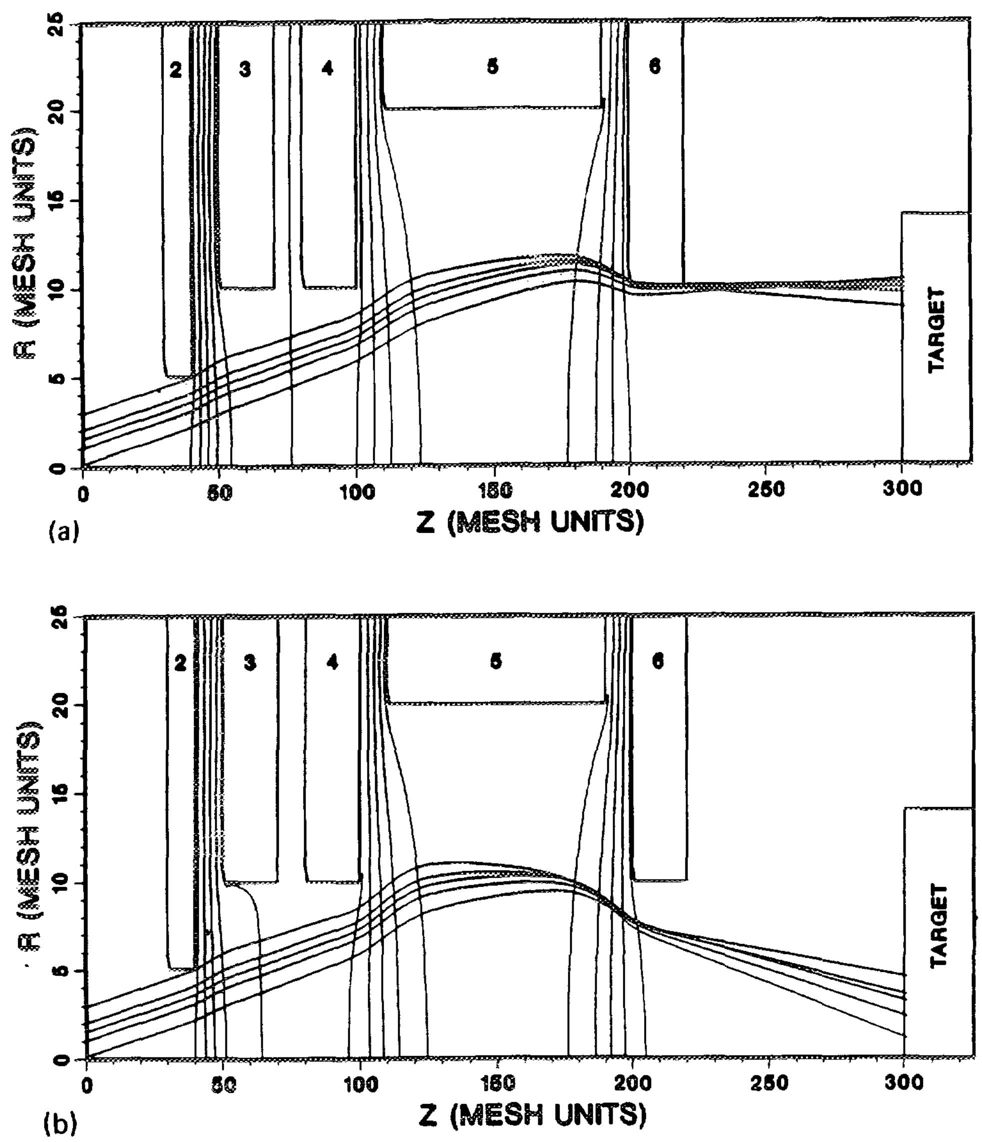

FIG. 5. Model plot of ray paths through decelerator of Fig. 3 for 1-keV-decelerated beam showing (a) beam contact with lens element 6 and (b) further focus attempt with no focusing on target.

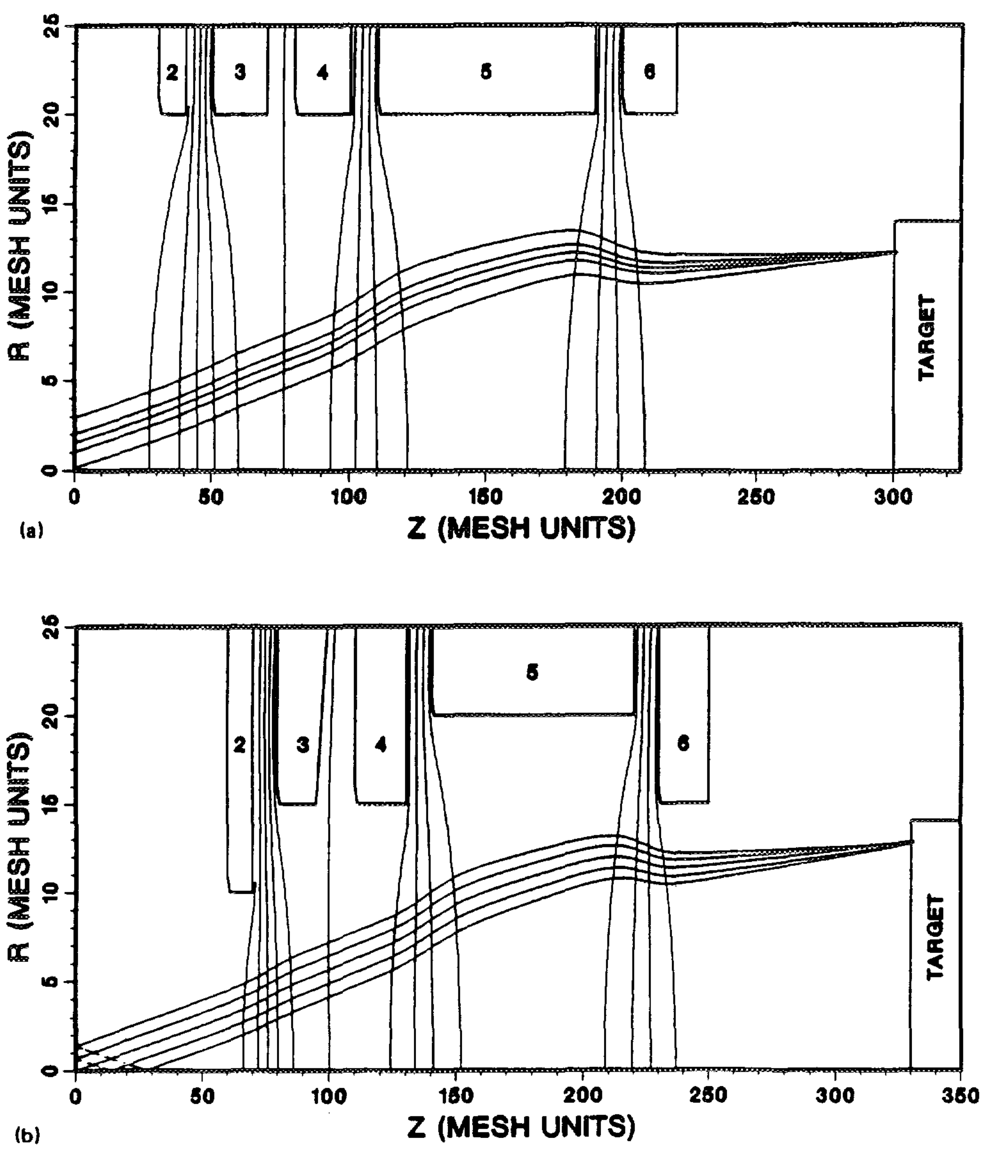

FIG. 6. Model plot of ray paths through decelerator with modified lens bore diameters showing good spot focus for (a) all lens element bore diameters enlarged and (b) final decelerator geometry.

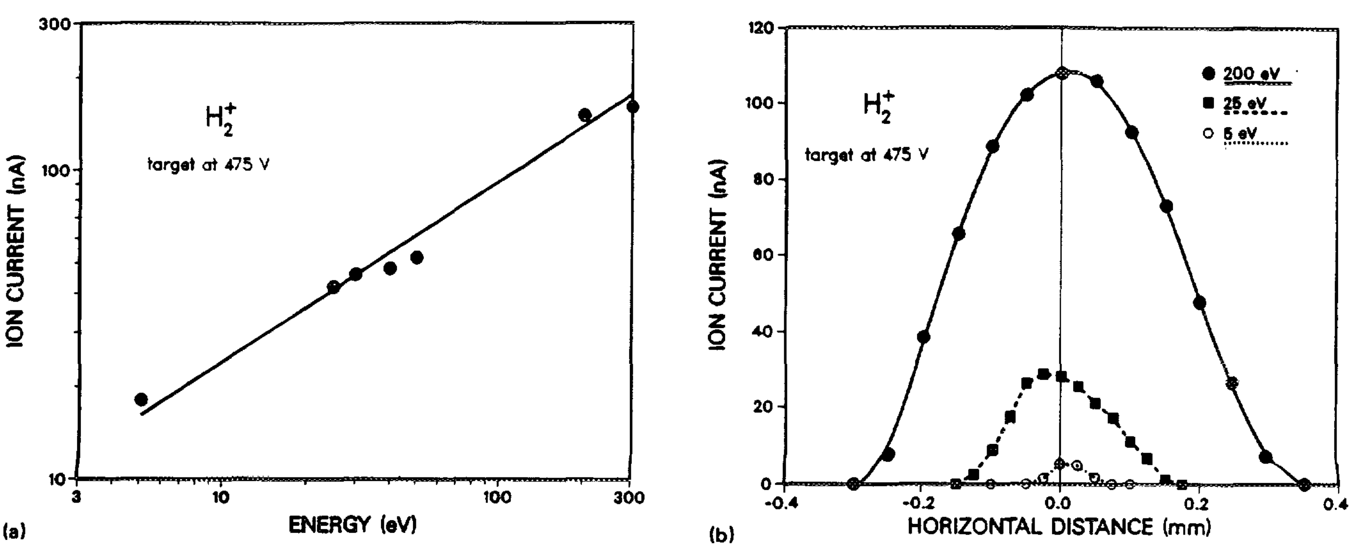

FIG. 7. Performance of decelerator with geometry of Fig. 6(b) showing (a) beam current vs decelerated beam energy with least squares fit and (b) typical beam profiles at selected beam energies (total current collected by scan wire probe).

typical but not necessarily optimized. Taken together, these results fully satisfy the low-energy beam requirements discussed in Sec. III.

VI. SUMMARY

An ion beam system with associated beam line optical components has been developed which produces a well-defined ion beam at low-incident energies. The beam is controllable in energy, ion species, focal properties, and effective spot size. Hydrogen ion beams at energies down to 5 eV and currents $\geqslant 20$ nA can be obtained, with a controllable spot size adjustable from tens of mm to <0.5-mm diameter using a beam raster system. The system is being used in experimental studies of low-energy ion/surface interactions and should be of general use in applications that require a well-characterized, low-energy ion beam.

ACKNOWLEDGMENTS

The authors would like to thank C. L. Bisson for many helpful discussions which facilitated our use of the electron trajectory code and to K. L. Black and J. A. Whaley for their technical assistance. One of the authors (BLC) acknowledges that the research was performed while under appointment to the Magnetic Fusion Energy Technology Fellowship program administered by Oak Ridge Associated Universities for the U. S. Department of Energy. DNR acknowledges the Presidential Young Investigators program of the National Science Foundation.This work was supported by the U. S. Department of Energy.

[1]R. A. Langley *et al.*, in "Data Compendium for Plasma–Surface Interactions," in *Nuclear Fusion* (IAEA, Vienna, 1984), special issue.
[2]K. L. Wilson, J. Nucl. Mater. **103**, 453 (1981).
[3]G. S. Oehrlein, Phys. Today, **39**, No. 10, 26 (1986).
[4]M. Menzinger and L Wåhlin, Rev. Sci. Instrum. **40**, 102 (1969).
[5]L. Wåhlin, Nucl. Instrum. Methods **27**, 55 (1964).
[6]R. Bastasz, IEEE Trans. Nucl. Sci. **30**, 1183 (1983).
[7]Menzinger Retardation System model 400, Colutron Research Corp., Boulder, CO.
[8]W. B. Herrmannsfeldt, Stanford Linear Accelerator Center Report No. SLAC-226, 1979.
[9]W. B. Herrmannsfeldt, Nucl. Instrum. Methods **187**, 245 (1981).